USE OF HIGH-RESOLUTION *ΔE-E* GAS IONISATION DETECTOR FOR THE $^{6}Li + ^{10}B$ SYSTEM

Presented BY

JOHN, Samuel Odumu Ogana[1,3]
Postdoctoral Research Fellow
samjoh2014@gmail.com

Co-Authors
Prof. John, Carter[2]
Prof. Usman, Iyabo[2]
Prof. Mathuthu, Manny[1]

[1]CARST North-West University, Mahikeng Campus, South Africa.
[2]School of Physics, University of the Witwatersrand, Johannesburg 2050, South Africa.
[3]Physics Department, Nasarawa State University Keffi, Nigeria.

1

CARST

NSRG

Gauteng

The 3rd African Conference on Fundamental and Applied Physics (ACP2023)
24-29 September 2023 at Nelson Mandela University, George, South Africa.

Presentation Outline

Introduction

Nuclear Scattering Reaction and *ΔE-E* Technique

Experimental Details

Results and Discussion

Summary and Conclusions

Potential Applications

Introduction

- The main sources of experimental information on nuclei structure, nuclear processes mechanisms and nucleus-nucleus interaction properties, are Nuclear Reaction.
- Varied set up and geometry leads to obtaining new experimental data, an urgent task in nuclear physics.
- The *ΔE-E* technique has proved a powerful tool in nuclear particles identification (McGrath, 1999 & Jingo, 2010).
- Identification of elements and isotopes by nuclear scattering reaction forms the basis of this work with potential application.
- The experiment was performed at iThemba LABS Gauteng, using the 6 MV EN Tandem accelerator through Nuclear Structure Research Group (NSRG), School of Physics, University of the Witwatersrand Johannesburg.

Nuclear Scattering Reaction and *ΔE-E* Technique

- The collision of two or more nuclear particles (projectile and target) results in nuclear scattering yielding ejectile and recoil nuclei in channels.
- Coulomb and Rutherford scattering describes elastic and inelastic scattering.
- An optical interaction potential across space separating the projectile and target nuclei is

$$U(r) = U_C(r) + U_N(r) \tag{1}$$

$$U_C(r) = \frac{Z_1 Z_2 e^2}{r}, \quad r > R_C \tag{2}$$

$$U_N(r) = V(r) + iW(r) \tag{3}$$

$$\left[\frac{d^2}{dr^2} + \frac{2\mu}{\hbar^2}(E - U(r)) - \frac{l(l+1)}{r^2}\right] f_l(r) = 0 \tag{4}$$

- *ΔE-E* technique operates on Energy Loss,

$$\Delta E = K\frac{MZ^2}{E} \tag{5}$$

- Bethe-Bloch equation describes the rate of energy loss of a charged particle by ionisation in a track for a given *ΔE* detector of thin gas-ionisation.

$$\frac{dE}{dx} = \frac{4\pi q^4 Z^2}{mV^2} Nz\left[ln\frac{2mV^2}{I} - \ln(1-\beta^2) - \beta^2\right] \tag{6}$$

Experimental Details

- The experiment's geometry is $^{6}Li + ^{10}B$, E_{Lab} (^{6}Li) = 20 MeV , θ_{Lab} = 35° , Lithium-6 ion ($^{6}Li^{3+}$, I = 45 nA) projectile; Boron-10 (Density of 200 $\mu g/cm^2$) target.
- C-Line alignment using ***Theodolite,*** switched on hours to a stable temperature before run.
- The gas delivery system use Iso-butane gas, operated at average differential pressure of 2.5 kPa, 56%. Safety checks, shutting down and up procedure observed before beam on.

Table 1: *ΔE-E* Detectors' Operating Conditions

Voltages (V)					Current (μA)		Gain
V_S	V_M	V_A	V_G	V_C	I_S	I_M	
+200	+170	+200	+30	- 30	0.31	0.21	1K – 500

- Best detectors' performance achieved for (V_G - V_C) = 60 V and (V_A - V_G) = 170 V.
- 6 Runs at average beam time of 3-7 hrs with high (1K) and low (500) gain was achieved.
- Preamps conveyed signals from detector to ADC connected to computer for signal processing.
- A computerised MIDAS multichannel online data acquisition system used, MATLAB for data analysis and CATKIN software for reaction Kinematics.

NWU®

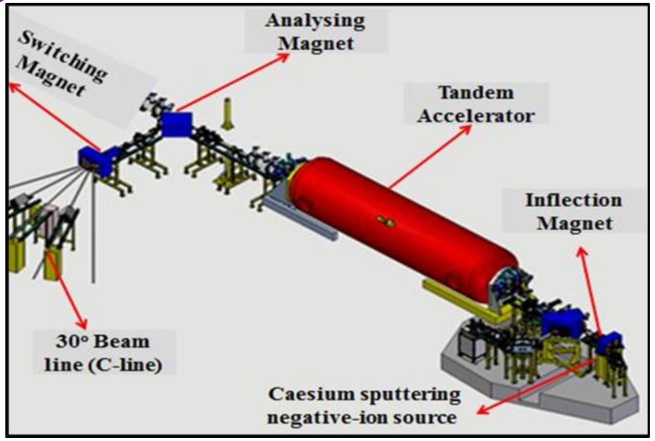

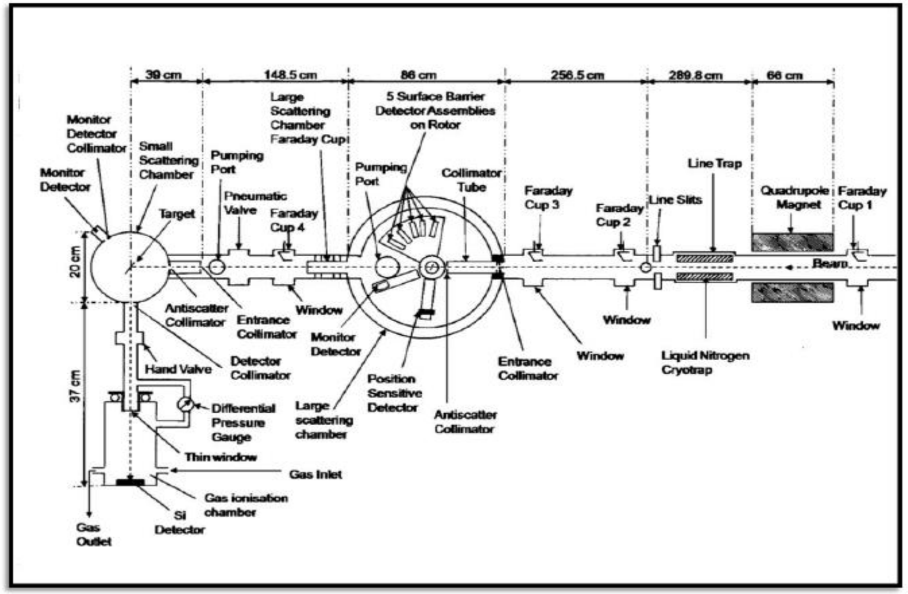

Fig. 1 : Schematic Lay-out of EN Tandem Van de Graaff Accelerator of iThemba LABS (Gauteng).

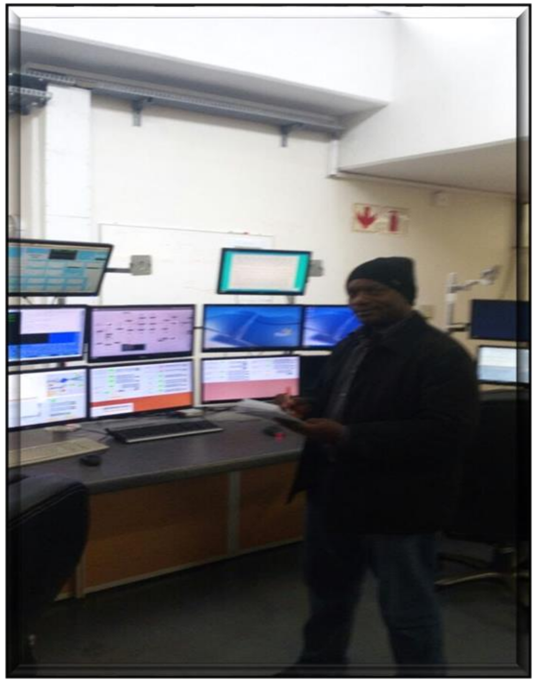

Beam time session with Prof. (Emeritus) JOHN Carter at iThemba LABS Gauteng S/Africa.

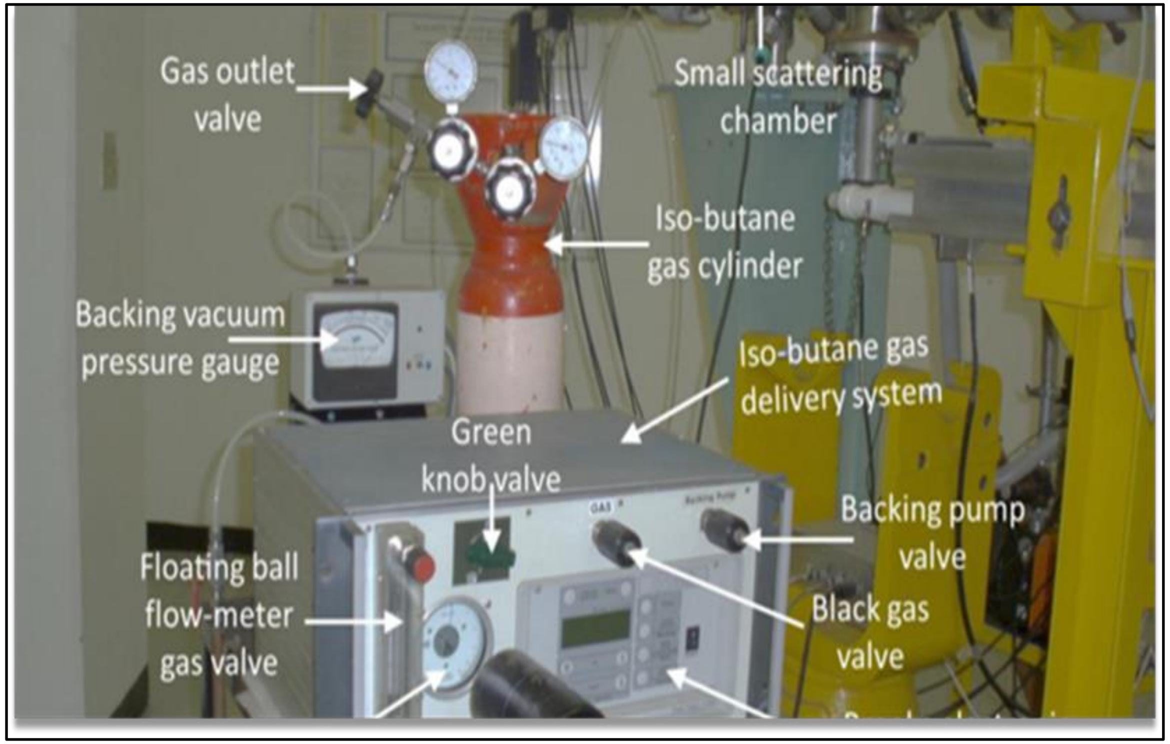

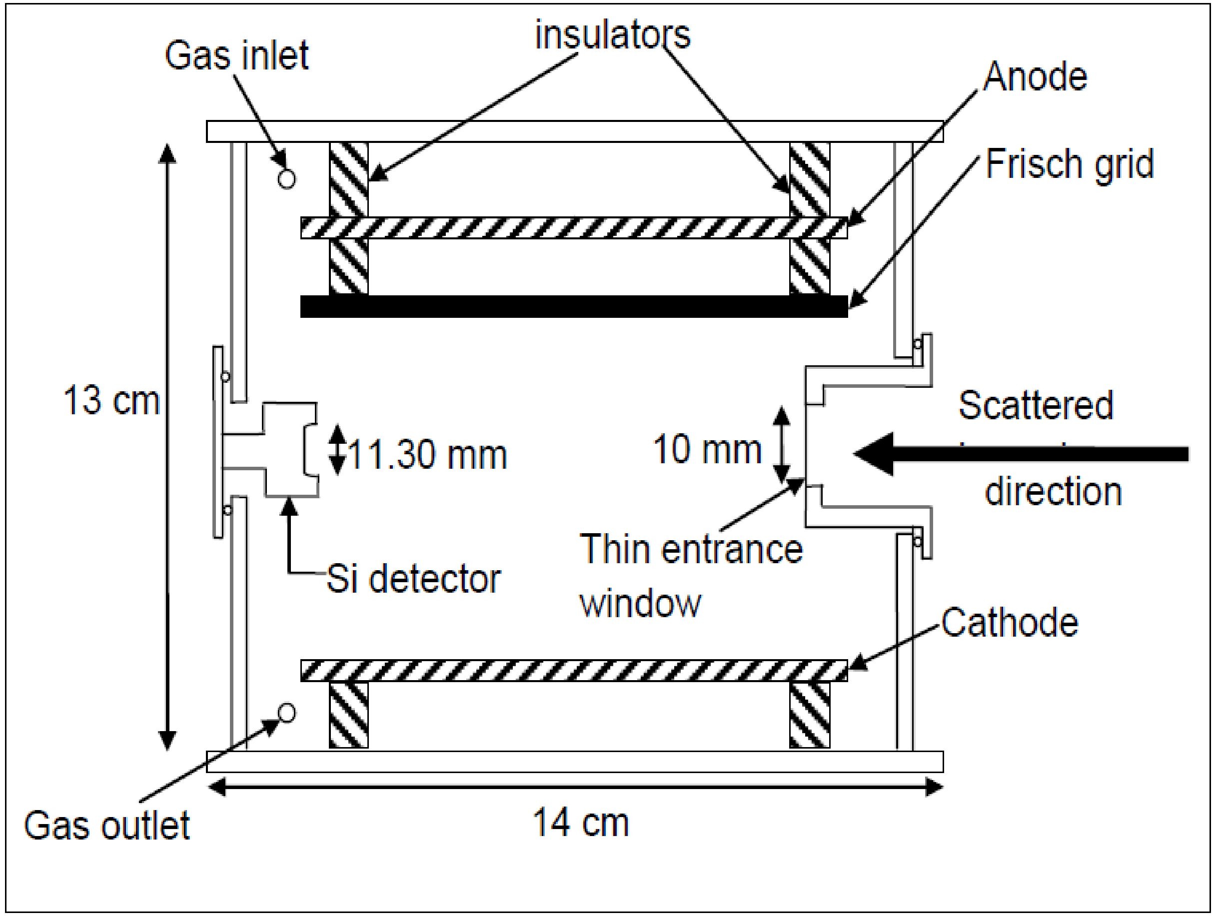

Fig. 2: Part of the Beam line picture of Gas delivery system and *ΔE-E* gas ionization detector schematic diagram.

Results and Discussion

- Total Kinetic Energy loss spectra for various transfer channels have been measured,
- The signal ΔE plotted against E_{Total}, n for High gain = 0.078, Low gain = 0.156 and from Eq. 7

$$E_{Total} = E_{stop} + n\Delta E \qquad (7)$$

- Calibration of energy spectra are determined by estimating which peaks correspond to known levels at accuracy of 30 – 50 KeV .
- The E – detector depletion depth is sufficient to stop 16 MeV protons.
- Particles with charge – one have typical peak widths for narrow residual levels.
- Peaks are assigned to energy levels given in the compilation by Tilley and Weller (1999), F. Ajzenberg-Selove (1990) from Nuclear Data Sheet.
- At peaks, 5-transfer reaction (inelastic scattering) as well as 5-scattering reactions (elastic) were obtained, Table 2, Figures 6 - 13.

Results and Discussion Contd.

Table 2: Reactions observed in the present experiment

S/N	Channel	*Q*-Value (MeV)	Type of scattering	Peak Energy (MeV)	Calibration (MeV/Ch)
1	$p(^{6}Li\ ,\ p)^{6}Li$	0	Elastic	6.593	0.023429
2	$p(^{6}Li\ ,\ ^{3}He)^{4}He$	4.020	Reaction	11.887	0.024062
3	$^{10}B(^{6}Li\ ,\ ^{3}He)^{13}C$	8.0803	Reaction	25.890	0.02328
4	$^{10}B(^{6}Li\ ,\ ^{4}He)^{12}C$	23.713	Reaction	39.336	0.024318
5	$^{10}B(^{6}Li\ ,\ ^{6}Li)^{10}B$	0	Elastic	15.974	0.025019
6	$^{16}O(^{6}Li\ ,\ ^{6}Li)^{16}O$	0	Elastic	17.423	0.024367
7	$^{28}Si(^{6}Li\ ,\ ^{6}Li)^{28}Si$	0	Elastic	18.495	0.023234
8	$^{10}B(^{6}Li\ ,\ ^{9}Be)^{7}Be$	- 0.980	Reaction	12.911	0.024509
9	$^{10}B(^{6}Li\ ,\ ^{10}B)^{6}Li$	0	Elastic	12.583	0.028532
10	$^{10}B(^{6}Li\ ,\ ^{12}C)^{4}He$	23.713	Reaction	11.503	0.029129

Results and Discussion Contd.

- **(a)**and **(c)** acquired at high gain 1K, **(b)** and **(d)** acquired at low gain 500.
- **(a)** and **(b)** with stop energy; **(c)** and **(d)** with total energy (applying Eq. 7)

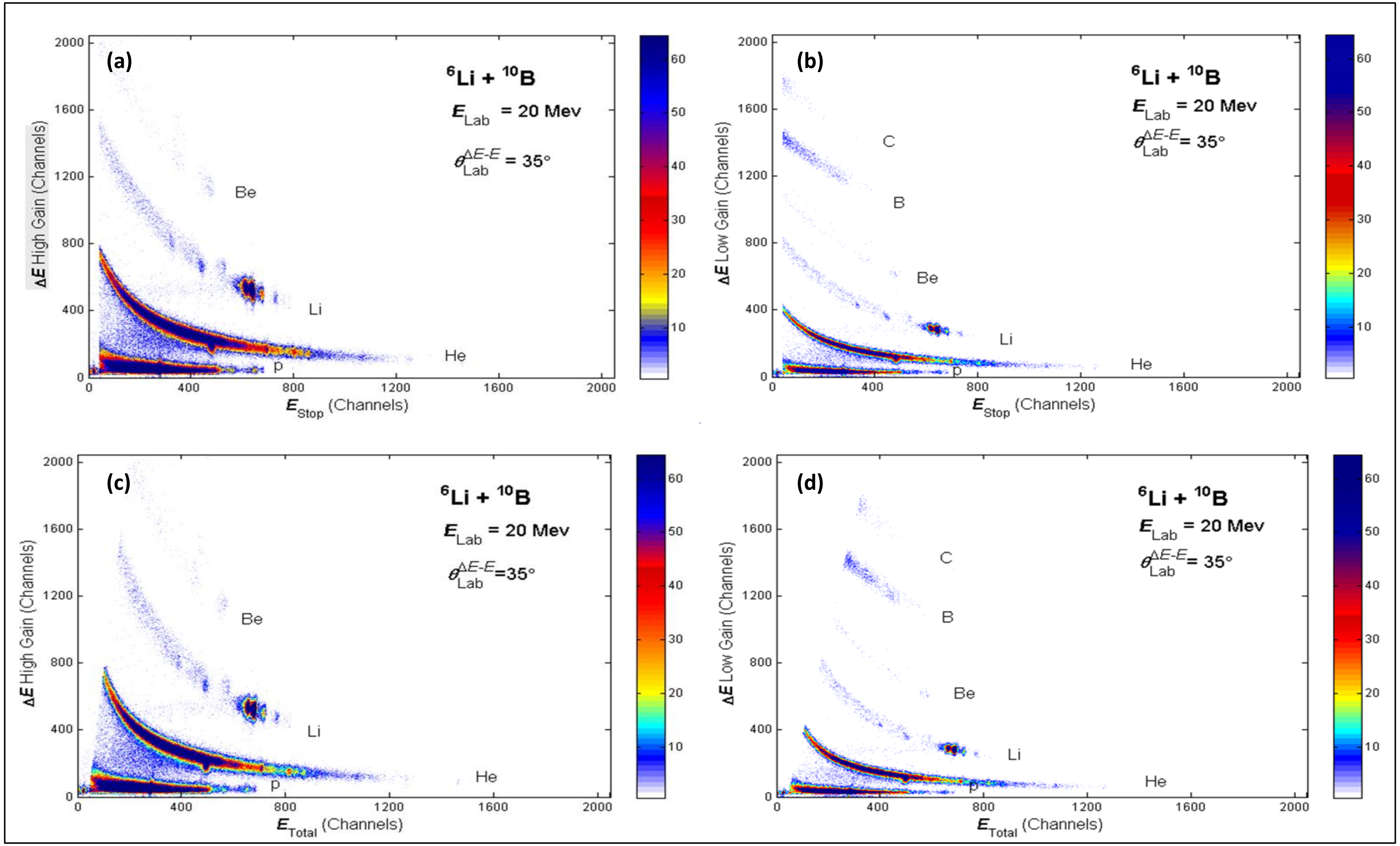

Fig. 6: 2-dimensional *ΔE-E* spectrum of ^{6}Li + ^{10}B reaction products showing projectile-like fragments

Results and Discussion Contd.

- The spectrum $Z = 1 - 4$ were observed only at high-gain.
- At low-gain, two additional spectrum were observed $Z = 5$ and 6.
- Lowering the gain open channel providing for more counts for higher Z to be observed.
- Comparison of the spectrum indicates channel shift as Z increases.

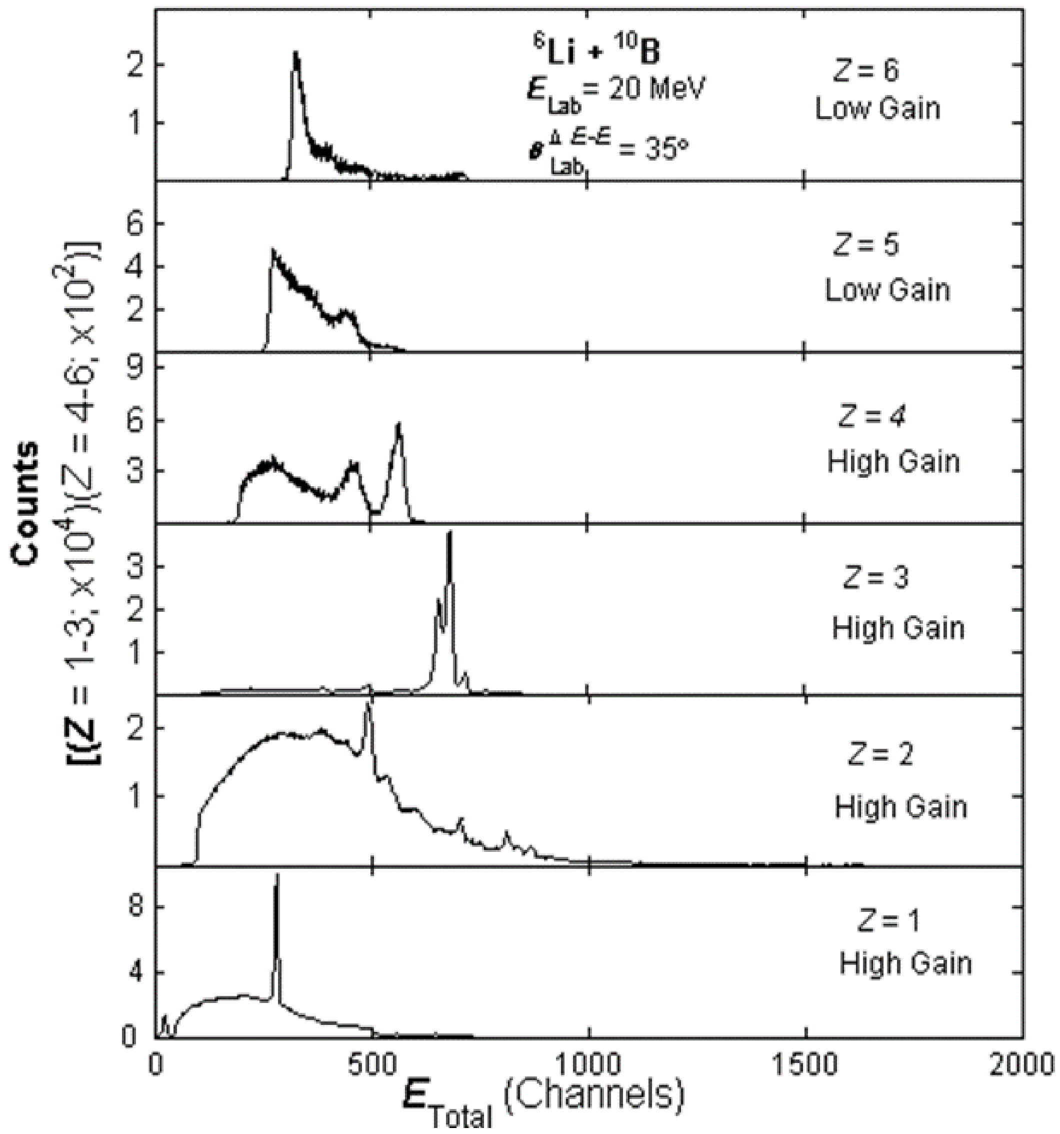

Fig. 7: 1-dimensional step-plot Energy(Channels) Spectra for each Isotope and Element

Energy Spectra (Z=1)

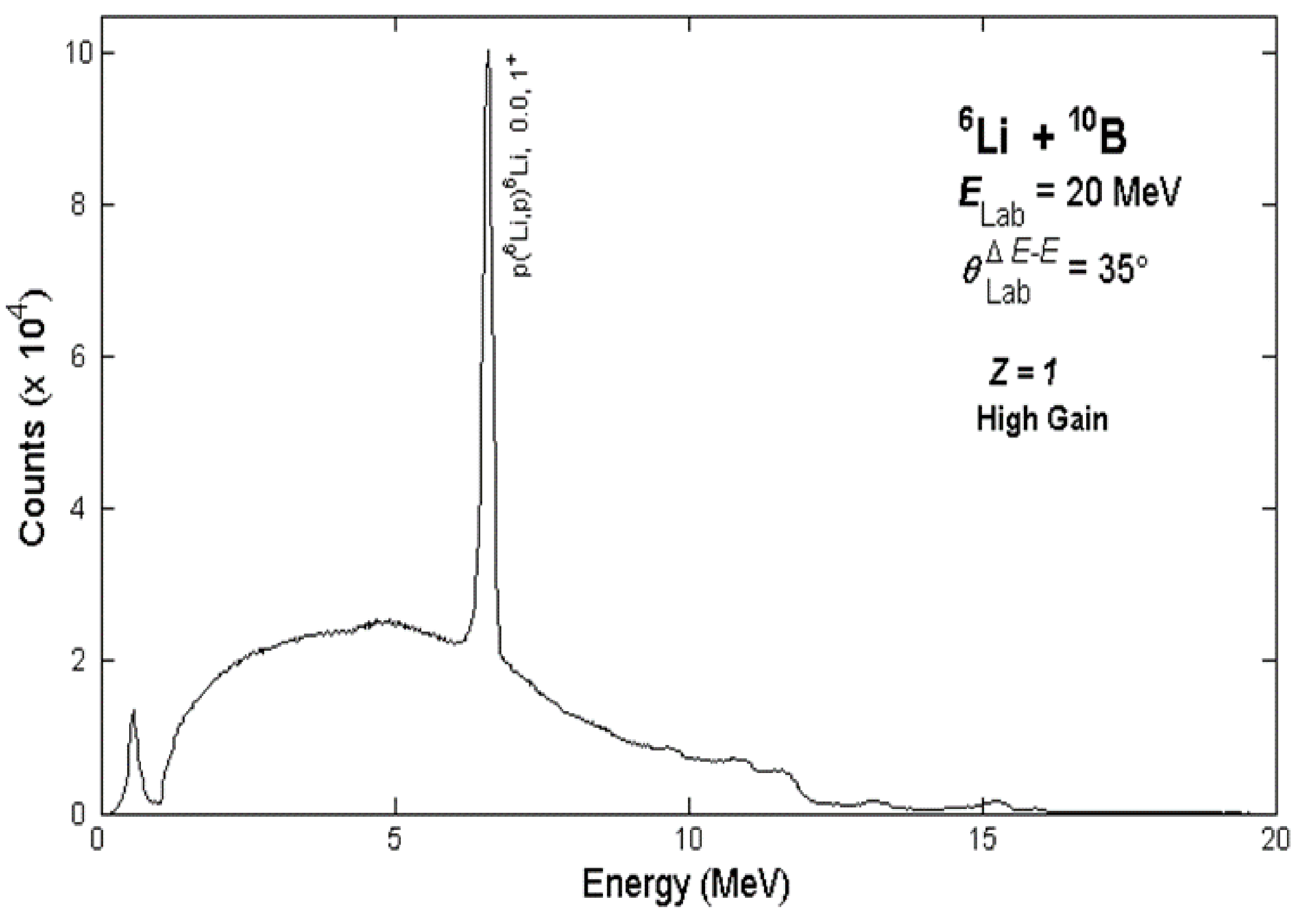

Fig. 8: 1-dimensional Spectrum for Proton (H) *Z* = 1, High Gain. Peak Energy in MeV

- Elastically scattered protons contaminating target caused the *Z* = 1 spectrum near low energy cutoff.
- 6.593 MeV corresponds to groundstate (0.0 MeV, 1^+ state) of ^{6}Li.
- Large continuum peaks from groundstate group of ^{15}N not observed.
- About 30 groups observed for E_{Lab} (^{6}Li) = 3.05 MeV, ϑ_{Lab} = 20^o (McGrath, 1966).
- Hydrogen (proton) peak identified.

Energy Spectra (Z=2)

- Proton contamination in the target produces p(^{6}Li , ^{3}He)^{4}He peak whose energy (11.887 MeV) corresponds to 0^+ groundstate of ^{4}He.
- 13 peaks from reaction ^{10}B(^{6}Li , ^{3}He)^{13}C whose energy corresponds to ground and excited states of ^{13}C are observed.
- The low energy peaks are due to H, ^{12}C and ^{13}C produced.
- 4 peaks correspond to ground and excited state of ^{12}C are observed, including Hoyle ground state.
- Helium isotopes ^{3}He, ^{4}He are identified.

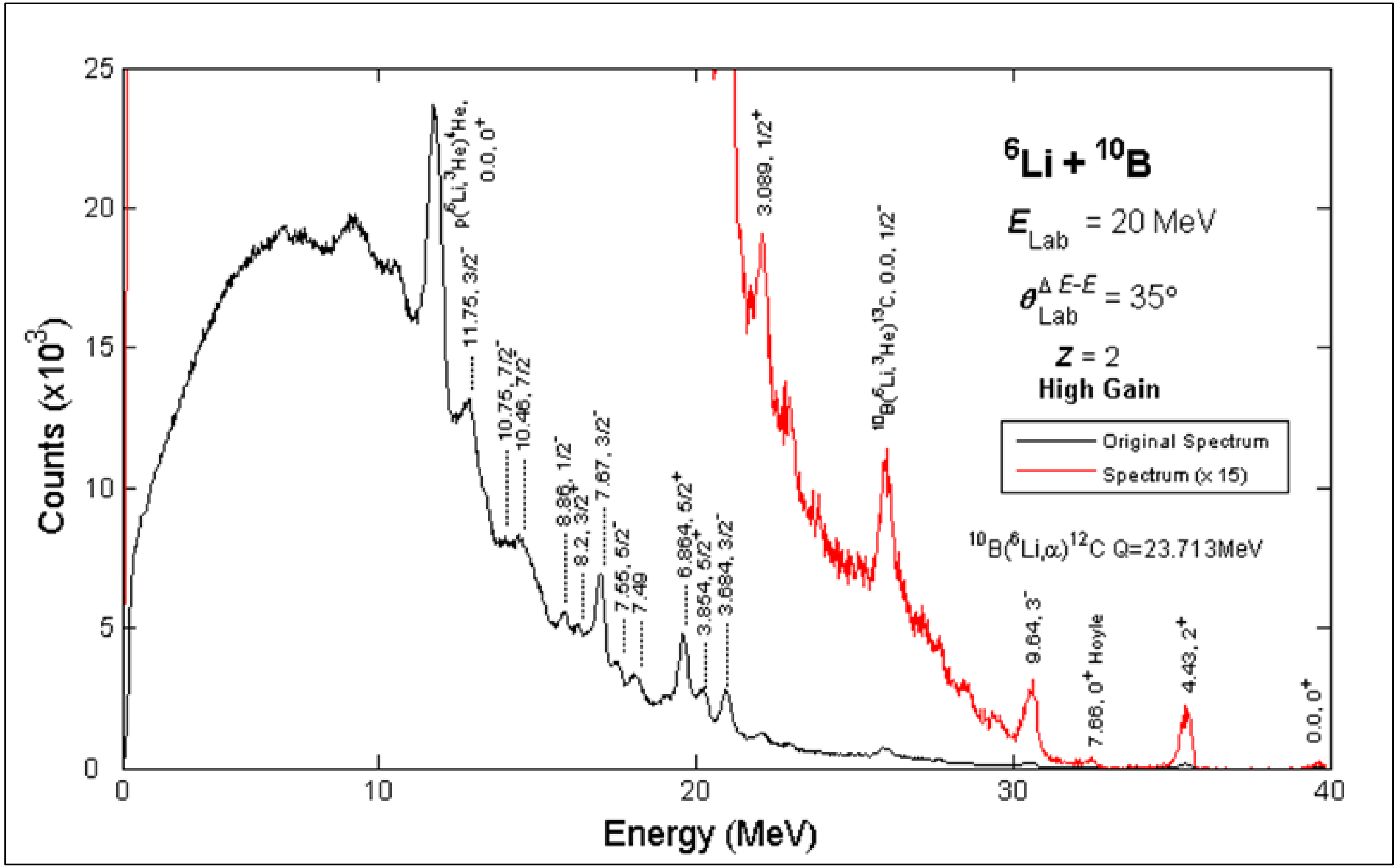

Fig. 9: 1-dimensional Spectrum for Alpha (He) *Z* = 2, High Gain. Peak Energy in MeV.

Energy Spectra (Z=3)

- Elastically scattered peak from $^{10}B(^{6}Li, {}^{6}Li)^{10}B$ of energy 15.974 MeV correspond to 3^{+} ground state and 6 excited states of ^{10}B are observed.
- Two elastically scattered peaks from ^{16}O and ^{28}Si contamination populated ^{6}Li at energy of 17.423 MeV and 18.495 MeV.
- Low energy peaks are due to contamination from oxygen and silicon.
- ^{6}Li energy spectrum peak identified but ^{7}Li not observed.
- Study on elastic scattering of $^{10}B(^{6}Li, {}^{6}Li)^{10}B$ reaction at $E_{Lab}(^{6}Li)$ = 5.8 MeV and 30 MeV also identified strong peak of ^{6}Li from ^{10}B (NNDC).

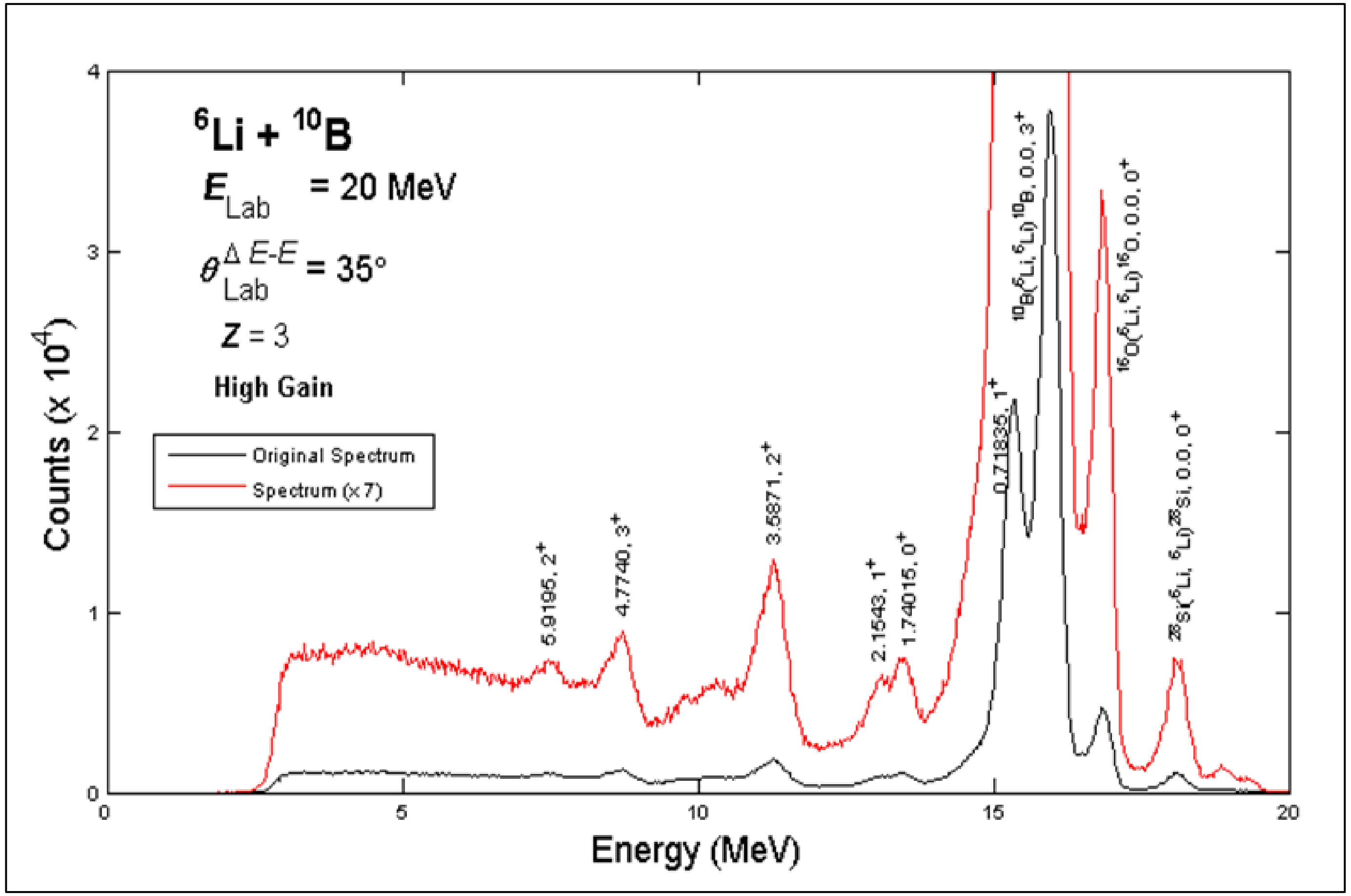

Fig. 10: 1-dimensional Spectrum for Lithium (Li) *Z* = 3 High Gain. Peak Energy in MeV

Energy Spectra (Z=4)

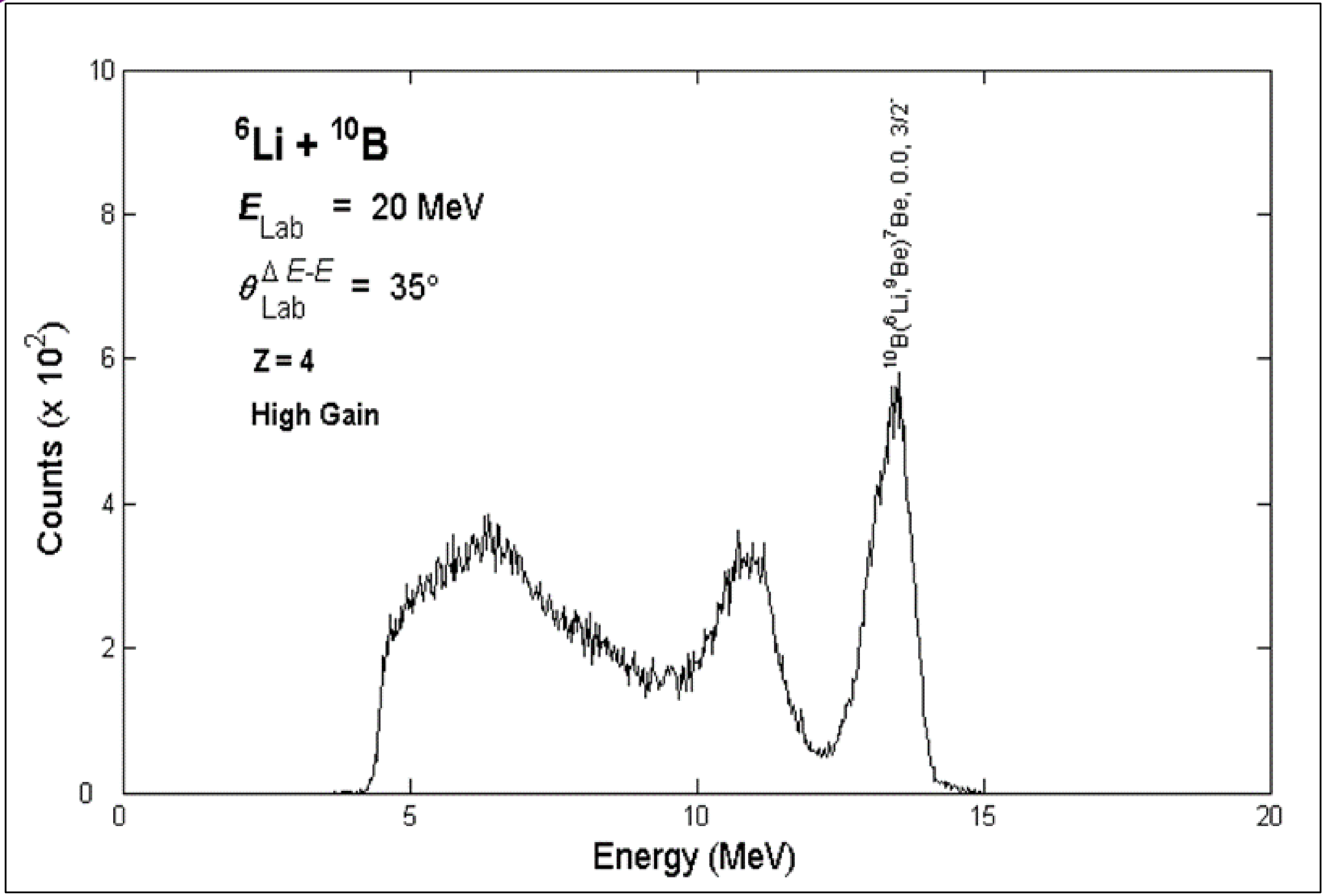

Fig. 11: 1-dimensional Spectrum for Beryllium (Be) *Z* = 4 High Gain. Peak Energy in MeV

- ^{9}Be is in-elastically populated from $^{10}B(^{6}Li, ^{9}Be)^{7}Be$ reaction with energy 12.911MeV, correspond to the $3/2^-$ ground state of ^{7}Be.
- The run with high-gain used in the spectra analysis.
- Low – count observed due to weak population of spectrum in the channel compared to $Z = 1 – 3$ spectra.
- ^{9}Be isotope identified.

Energy Spectra (Z=5)

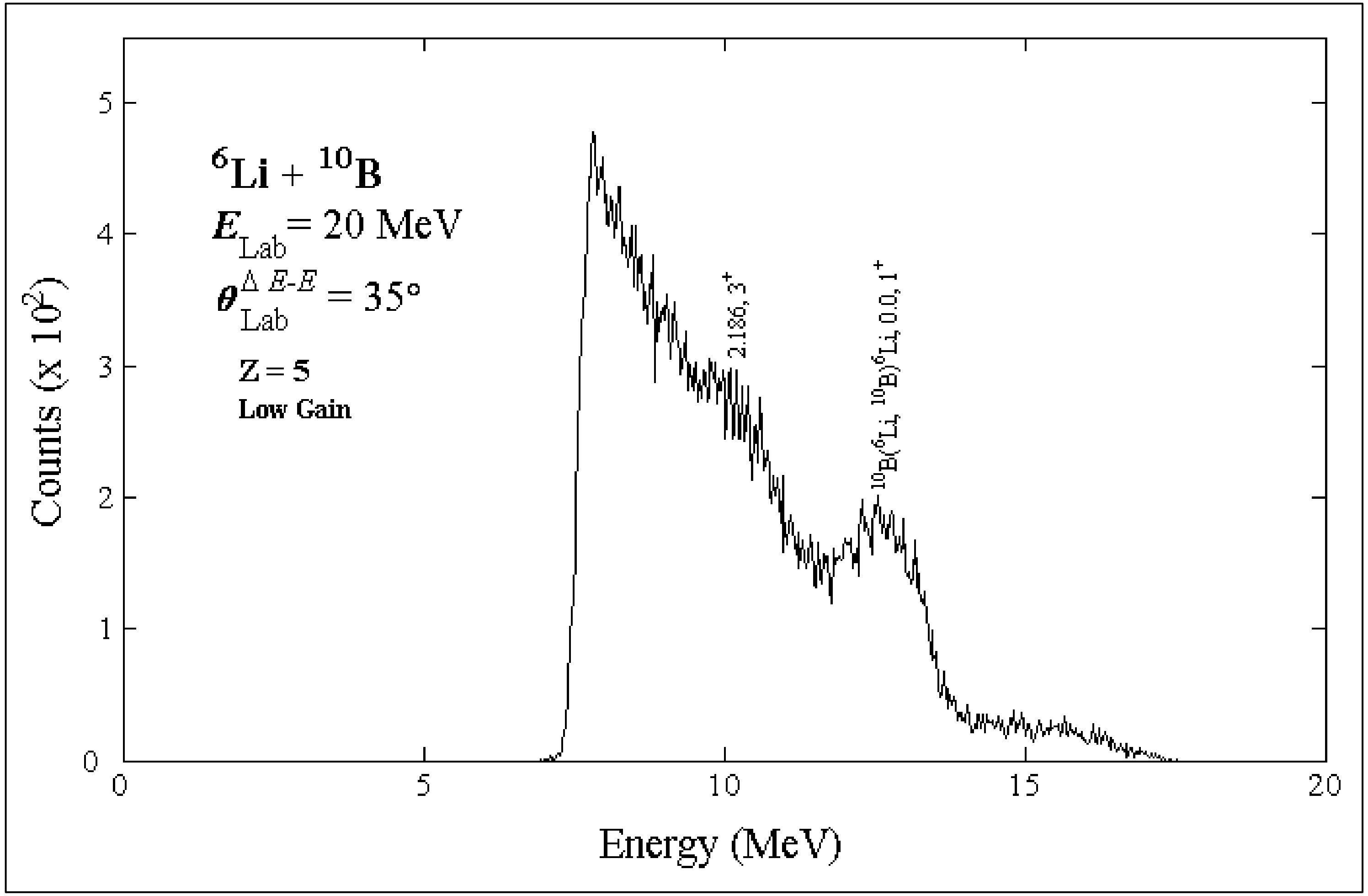

Fig. 12: 1-dimensional Spectrum for Boron (B) *Z* = 5 Low Gain. Peak Energy in MeV

- ^{10}B isotope weakly populated from elastic scattering reaction $^{10}B(^{6}Li, {}^{10}B)^{6}Li$. at energy 12.583 MeV, correspond to 1^{+} ground state and 3^{+} excited state of ^{6}Li.
- Low count observed possibly due to reaction geometry which favoured high population of *Z* = 1 – 3 channels.
- The Boron, *Z* = 5 spectrum was observed only at low-gain run.
- ^{10}B isotope identified.

Energy Spectra (Z=6)

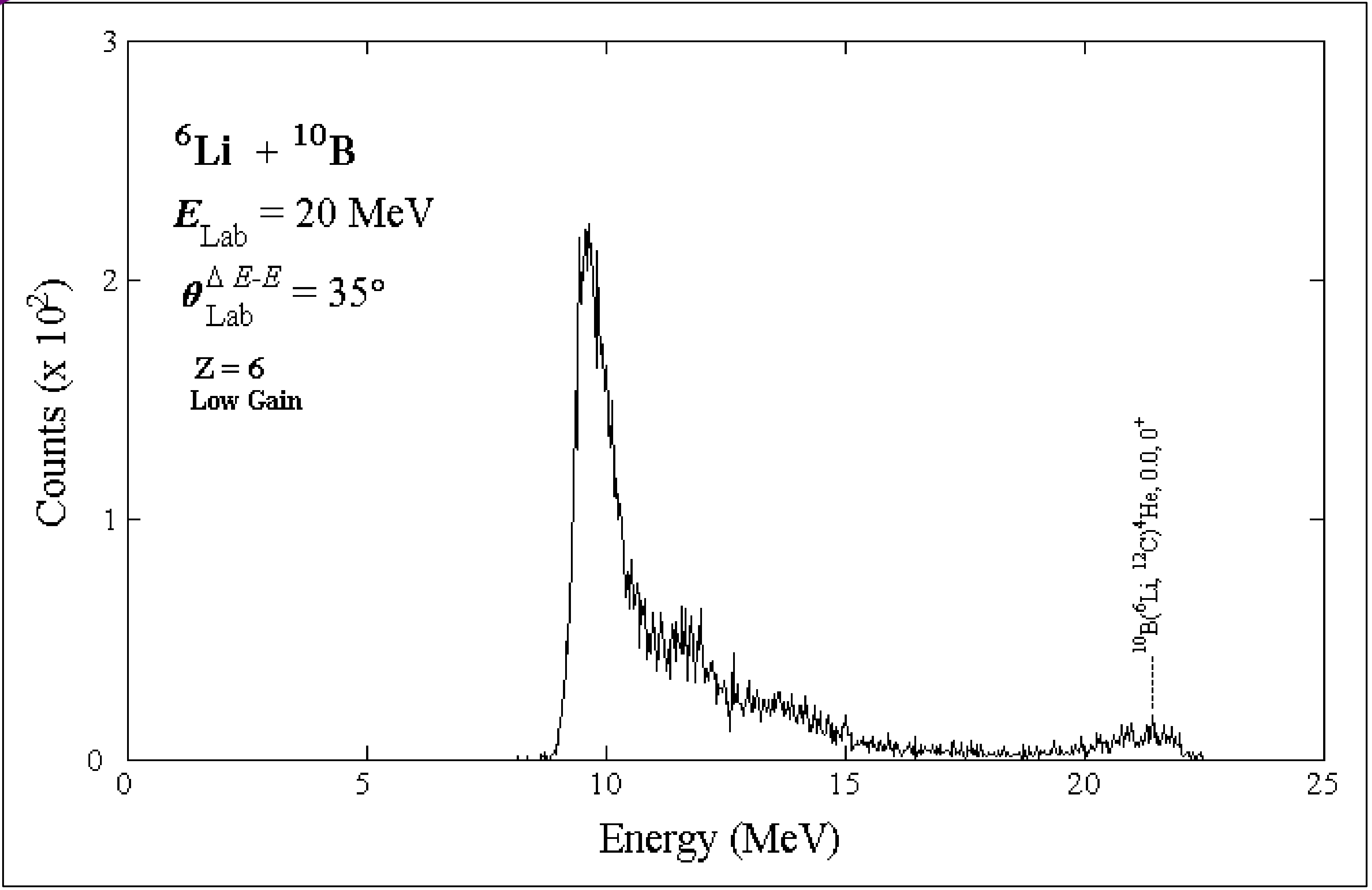

Fig. 13: 1-dimensional Spectrum for Carbon (C) *Z* = 6 Low Gain. Peak Energy in MeV

- ^{12}C is weakly populated from in-elastic scattering reaction at energy 11.503 MeV, corresponding to the 0$^+$ ground state of ^{4}He, with no excited state corresponding peak.
- The Carbon spectrum is only observed at low-gain run.
- ^{12}C isotope identified

Energy Level Diagrams

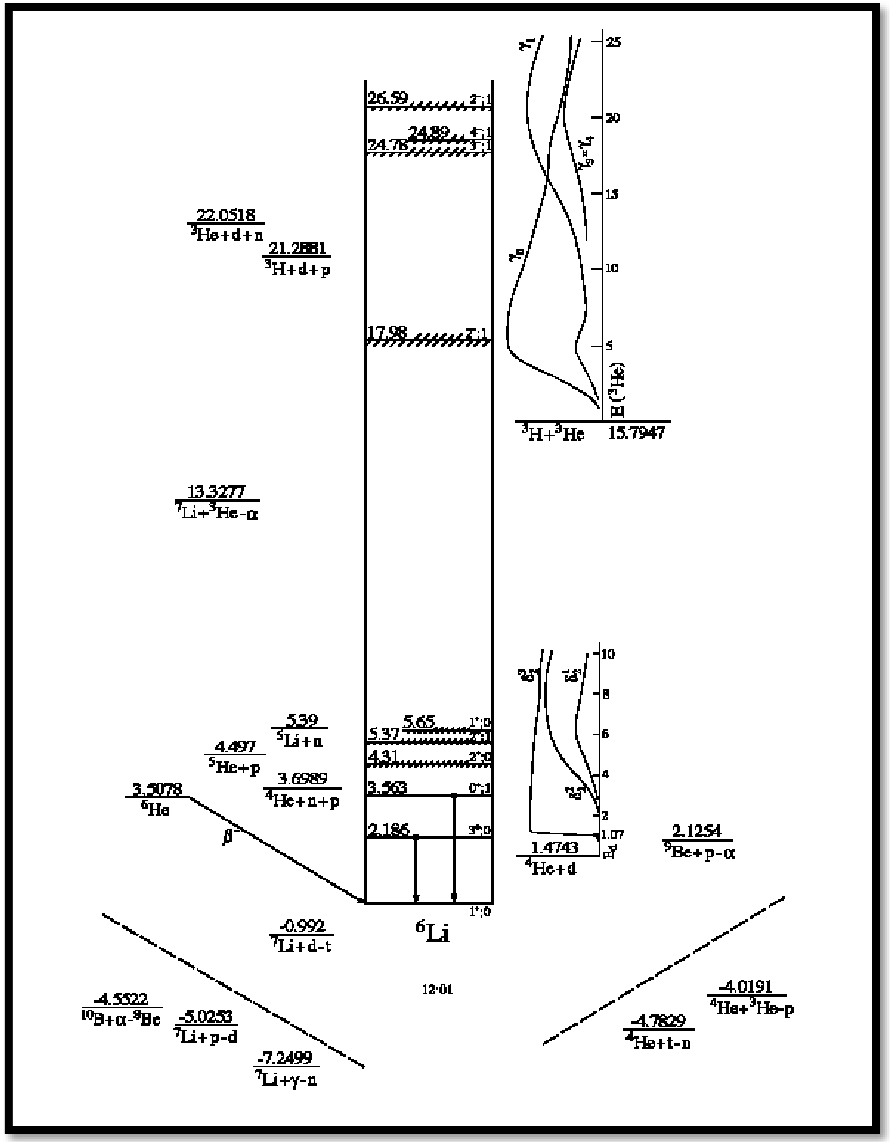

Lithium-6

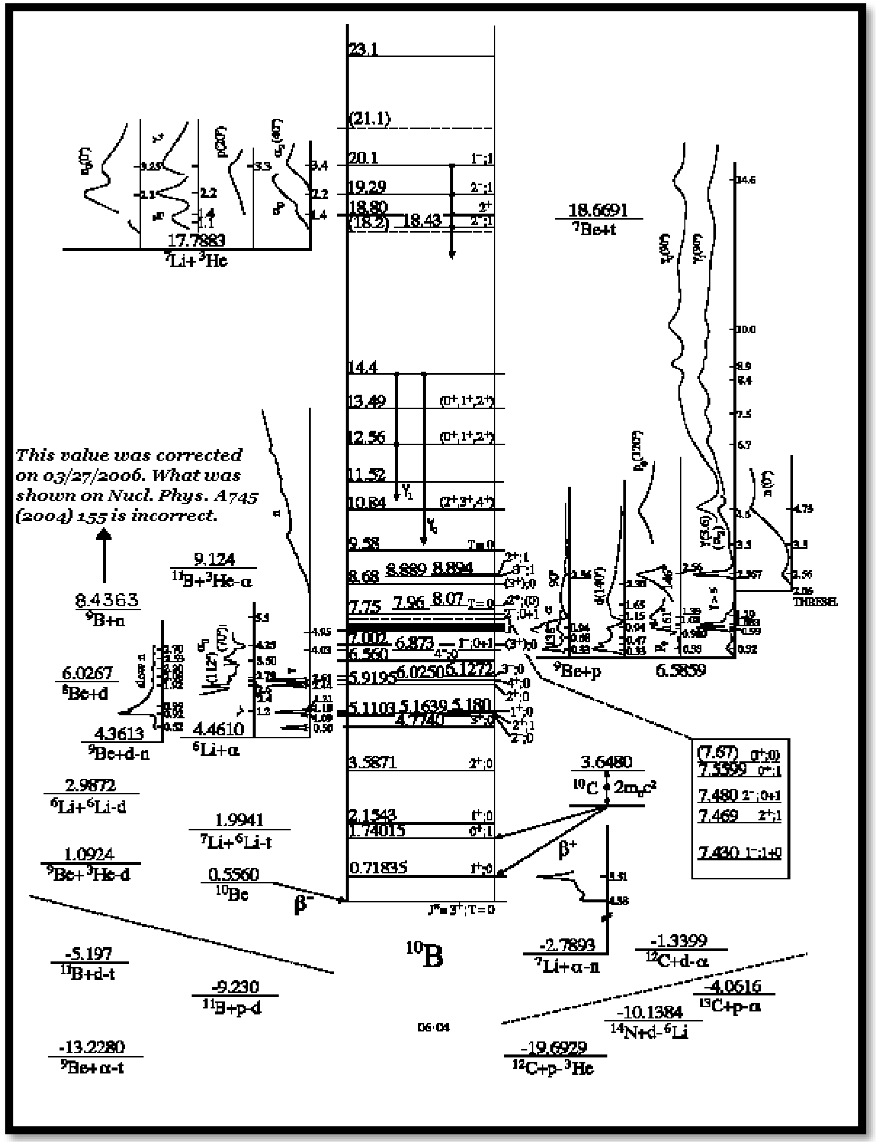

Boron-10

Energy Level Diagrams

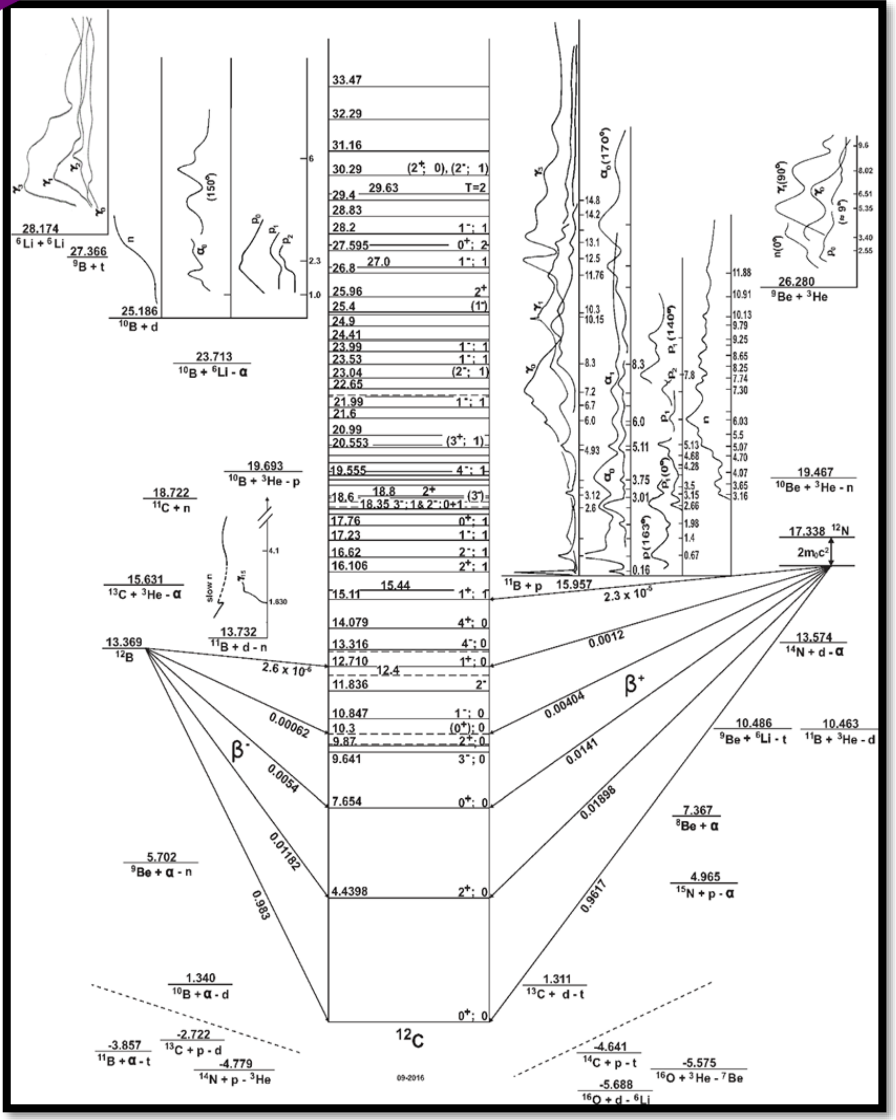

Carbon-12

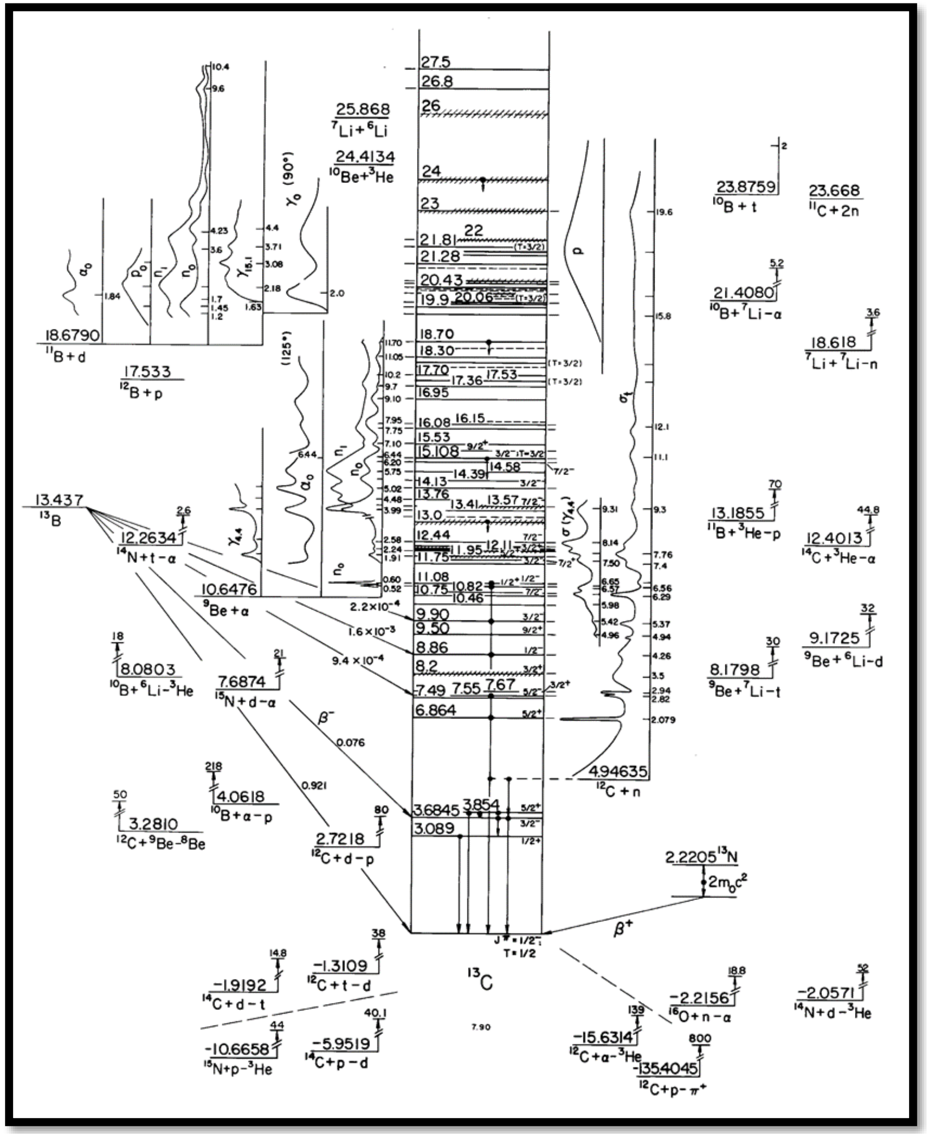

Carbon-13

Summary and conclusion

- The scattering ^{6}Li + ^{10}B reaction experiment was performed using the 6 MV EN Tandem Accelerator of iThemba LABS Gauteng.
- Due to high energy resolution of *ΔE-E* gas ionization detector, coupled with effective electronic system and geometry E_{Lab} (^{6}Li) = 20 MeV, ϑ_{Lab} = 35°, led to Low-*Z* elements and isotopes were identified such as: protons ($^{1}_{1}\mathrm{H}$), $^{3}_{2}\mathrm{He}_{1}$ and $^{4}_{2}\mathrm{He}_{2}$, $^{6}_{3}\mathrm{Li}_{3}$, $^{9}_{4}\mathrm{Be}_{5}$, $^{10}_{5}\mathrm{B}_{5}$, $^{12}_{6}\mathrm{C}_{6}$ and $^{13}_{6}\mathrm{C}_{7}$.
- Cross – section of the reaction can further be determined which will provide more information on the nuclear properties.

Potential Applications

- Provide experimental information on the parameters describing the structure of nuclei, mechanism of nuclear reaction and nucleus-nucleus interaction.
- Validate the use of high resolution ΔE-E spectrometer technique in charged particle energy discrimination and identification at a geometric condition.
- Provide experimental base to confirm the prediction of a 2^+ excited state 2 MeV above the Hoyle state.
- Applied to production of isotopes in industry, agriculture, medical, etc.
- Protons, High-Let Sources and Boron Neutron Capture Therapy

ACKNOWLEDGEMENT

NSRG

CARST

Thank you for listening

NWU

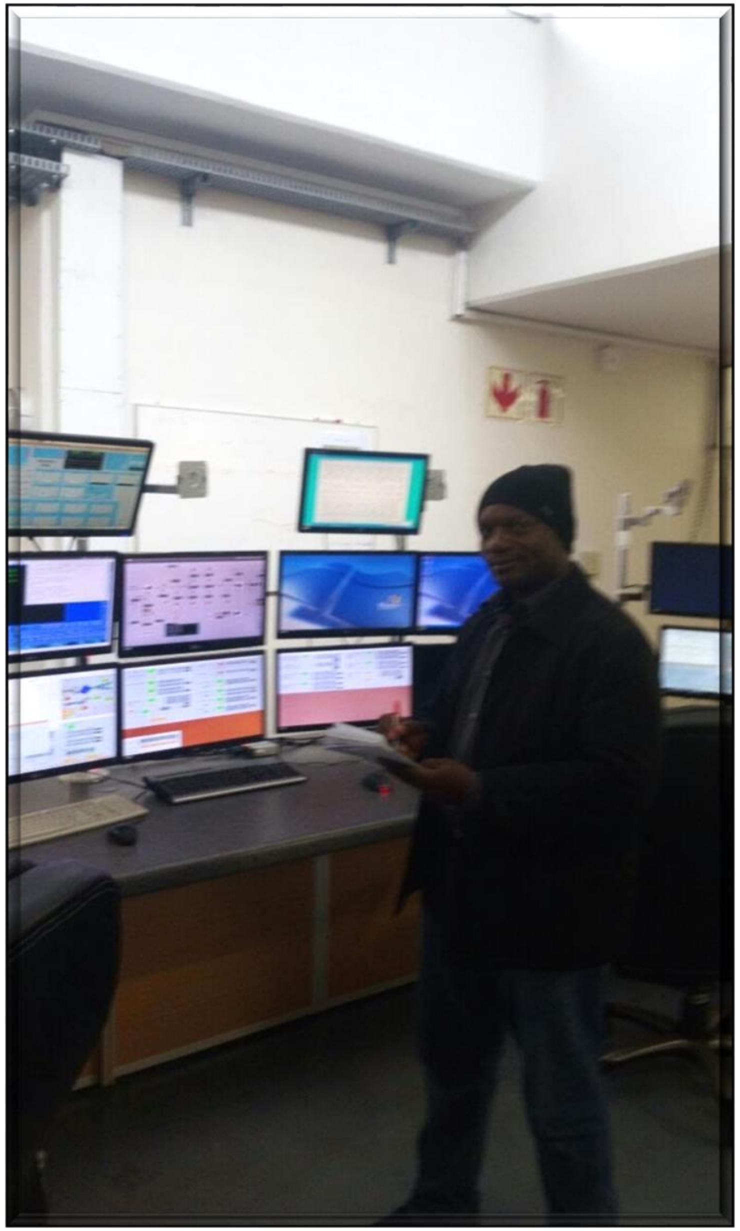

Beam time session with Prof. (Emeritus) JOHN Carter at iThemba LABS Gauteng S/Africa.